Chapter

The Use of Stable Isotope Labeling with Amino Acids in Cell Culture (SILAC) to Study Ivermectin-Mediated Molecular Pathway Changes in Human Ovarian Cancer Cells

Na Li and Xianquan Zhan

Abstract

Stable isotope labeling with amino acids in cell culture (SILAC) was to use isotopic essential amino acids to replace the original amino acids for cell culture and passage for 8–10 generations, followed by mass spectrometry to identify proteins and the isotopic abundance difference to quantify proteins. SILAC can be used to characterize proteomic changes, and analyze protein turnover, protein interactions, and dynamic changes with quantitative accuracy, and high reproducibility. For this study, SILAC "light" (L-Lysine-2HCl [^{12}C6, ^{14}N2], L-Arginine-HCl [^{12}C6, ^{14}N4])- or "heavy" (L-Lysine-2HCl [^{13}C6, ^{15}N2], L-Arginine-HCl [^{13}C6, ^{15}N4])-labeling RPMI 1640 medium was used to culture human ovarian cancer TOV-21G cells for 10 passages, followed by the treatment of 0.1% dimethylsulfoxide for 24 h and 20 μM ivermectin for 24 h, respectively. The light- and heavy-isotope-labeled proteins were equally mixed (1:1) for digestion with trypsin. The tryptic peptide mixture was fractionated with liquid chromatography and analyzed with tandem mass spectrometry. In total, 4,447 proteins were identified in ivermectin-treated TOV-21G cells in relation to controls. Those proteins were enriched in 89 statistically significant signaling pathways and 62 statistically significant biological processes. These findings clearly demonstrated that SILAC quantitative proteomics was a useful and reliable method to study ivermectin-related proteomic changes in cancer cells, which in combination with molecular pathway networks and biological processes enrichments provided more comprehensive insights into molecular mechanisms of ivermectin in inhibiting TOV-21G cells.

Keywords: stable isotope labeling with amino acids in cell culture (SILAC), ovarian cancer, ivermectin, quantitative proteomics, bioinformatics analysis, molecular pathway, network, biological processes, biomarkers

1. Introduction

Stable isotope labeling with amino acids in cell culture (SILAC) is a polypeptide-labeling technology developed by the Thermo Fisher company of the United States in 2002 [1]. Heavy isotopes (^{13}C or ^{15}N) and light isotopes (^{12}C or ^{14}N) are used to label two essential amino acids (L-lysine and L-arginine) that are contained in a cell-cultured medium, respectively. After the cells were cultured with essential amino acids for 6–10 generations, all proteins were labeled with heavy isotopes or light isotopes. The cellular proteins stimulated by different treatment factors are analyzed by mass spectrometry (MS) to obtain the qualitative and quantitative proteome data [2]. SILAC generally allows heavy and light isotopes-labeled sample cells at the early stage of the experimental workflow, so the variability caused by the sample handling process was minimized [3]. SILAC was widely used in quantitative proteomics to study pathogenesis, drug target, protein modification and dynamics, protein-molecule interaction, and screen special functional proteins [4]. SILAC showed outstanding performance for quantification and dynamics of phosphosites in colorectal cancer with the treatment of the epidermal growth factor receptor (EGFR)-blocking antibody cetuximab, rendering it the effective method for cellular signaling study in cell culture models [5]. In terms of identification of protein-molecule interaction, SILAC combined with various affinity purifications of protein experimental setups could be used to distinguish specific complexes from nonspecific ones [6]. One study performed SILAC to overcome the most challenging problem in defining specific partners in protein complexes. The cells containing an affinity tagged protein were cultured in a light isotopic medium, while wild-type cells were grown in a heavy isotopic medium. The results of MS showed that specific partners appear as isotopically light [7]. SILAC also offers numerous opportunities to discover potential biomarkers and therapeutic targets for some drugs [8]. SILAC in combination with other developed approaches made SILAC more popular; for example, these SILAC labels in pulse or pulse-chase scenarios could be used to measure macromolecular dynamics on time scales of several hours [9]. An MS-based approach combining dynamic-SILAC labeling with isobaric mass tagging was well used to understand protein degradation and synthesis in cellular systems [10]. SILAC provided an effective scheme to comprehensively and systematically qualify and quantify complex mammalian cell proteome, which would promote progress in the medical field.

Ivermectin, marketed in 1981, was commonly used as a broad-spectrum anti-parasitic compound. It was approved to treat onchocerciasis (150–200 μg kg^{-1} body weight), scabies (200 μg kg^{-1} body weight), lymphatic filariasis (150–200 μg kg^{-1} body weight), demodicosis (200 μg kg^{-1} body weight), strongyloidiasis (200 μg kg^{-1} body weight), pediculosis (400 μg kg^{-1} body weight), and filariasis (due to Mansonella ozzardi, 6 mg as a single dose) [11].

Because ivermectin mainly targets chloride-dependent channels (γ-aminobutyric acid and glutamate), its safety could be fine in higher animals. In humans, especially the blood-brain barrier can reduce ivermectin delivery to the central nervous system [12]. The safety of ivermectin has been proved with clinical studies on children, infants, and pregnant women. A study including 170 infants and children with the treatment of oral ivermectin (mean dose = 223 μg kg^{-1}) showed good tolerance, and only seven subjects occurred mild adverse events [13]. A study including 893 pregnant women with the oral treatment of ivermectin also showed good tolerance, and no patients were reported to generate serious events (stillbirths, neonatal death, low birth weight, spontaneous abortions, preterm births, and congenital anomalies) [14]. Those studies proved that ivermectin was safe enough to be used in human diseases, but there was still insufficient evidence

to prove no adverse side effects. The highest ivermectin dose was 200 μg/kg, which was approved by FDA. However, some patients without serious events have used 10 times more than the FDA-approved dose [15]. All those made ivermectin more likely to achieve success in clinical application. In recent days, studies found that ivermectin was effective in a completely new range of diseases, such as neurological disorders, antiviral (e.g., dengue, HIV, and encephalitis), antibacterial (e.g., Buruli ulcer and tuberculosis), anticancer (melanoma, lymphoid leukemia, lung cancer, glioblastoma, and breast cancer) [11]. The functions and mechanisms of ivermectin on anticancer generated interest and excitement in the scientific community. Ivermectin suppresses breast cancer by disrupting cellular signaling in the process and activating cytostatic autophagy through mediating PAK1 expression [16]. Ivermectin showed a synergistic effect with the chemotherapy agents by increasing cell death in leukemia cells. Some researchers, who aimed at overcoming cancer, claimed that ivermectin could be rapidly advanced into clinical trials [17]. Further study on molecular network, signaling pathway, and key biological processes of ivermectin would provide more useful information about this multifaceted "wonder" drug.

This chapter describes that SILAC identifies differentially expressed proteins (DEGs) in ivermectin-treated ovarian cancer cells in the following aspects: (i) ovarian cancer cell culture—TOV21G and labeled with heavy and light SILAC reagents; (ii) ivermectin treatment of SILAC-labeled TOV21G cells and protein preparation; (iii) the quality of SILAC-labeled protein samples with 1D SDS-PAGE; (iv) trypsin-digestion of SILAC-labeled proteins; (v) each fraction was subjected to LC-MS/MS analysis; and (vi) bioinformatics analysis (signaling pathway and biological process). SILAC can be a useful and effective method to detect protein alterations and dynamic changes in living cells, and the results would provide scientific data to further clarify molecular mechanisms of ivermectin in ovarian cancer.

2. Methods

2.1 Ovarian cancer cell culture

The human ovarian cell line (TOV-21G) was cultured in RPMI 1640 medium supplemented with 10% fetal bovine serum (FBS) and 5% CO_2 at 37°C. (i) Ovarian cell line used here was TOV-21G, which was obtained from Keibai Academy of Science (Nanjing, China) [18]. (ii) RPMI 1640 was used without glutamine, lysine, and arginine. (iii) FBS was brought from Gibco® Certified Thermo Fisher Scientific. (iv) The growing states of TOV-21G were observed, and the medium was changed in every 2 days.

2.2 SILAC medium preparation and labeling

SILAC "light" or "heavy" labeling growing medium (Thermo Fisher Scientific, US) was used to culture TOV-21G cells for 10 passages, to ensure a high level of stable isotope replacing original amino acids [8]. (i) "Light" labeled amino acids: 50 mg L-arginine HCl (Arg0), 50 mg L-lysine HCl (Lys0). "Heavy" labeled amino acids: 50 mg L-arginine-^{13}C6,^{15}N4 HCl (Arg10), 50 mg L-lysine-^{13}C6,^{15}N2 HCl (Lys8). (ii) A total of 1 L RPMI 1640 without glutamine, lysine, and arginine. (iii) For SILAC experiments, 50 mg Arg0 and 50 mg Lys0 ("light" labeling reagent) were added into 500 mL RPMI 1640 medium to form SILAC "light" labeling growing medium. A total of 50 mg Arg10 and 50 mg Lys8

("heavy" labeling reagent) were added to 500 mL RPMI 1640 medium to form SILAC "heavy" labeling growing medium. (iv) The growing states of TOV-21G were observed, and the medium was changed in every 2 days. TOV-21G cells were cultured and passaged for 10 generations in 10-cm culture flasks.

2.3 Ivermectin treatment of SILAC-labeled TOV21G cells

When SILAC-labeled TOV21G cells achieved 80% cell density in 10-cm culture flasks, 20 μM ivermectin was added to TOV-21G cells in SILAC "heavy" labeling growing medium, and 0.1% DMSO was added to TOV-21G cells in SILAC "light" labeling growing medium for 24 h [19]. (i) Ivermectin ($C_{48}H_{74}O_{14}$, purity ≥ 95%): The drug was brought from Solarbio (http://www.solarbio.com/goods-3911.html). (ii) TOV-21G cells were counted, and 8000 cells/well were seeded in 96-well plates. Ivermectin was added into each well in different drug concentrations (0 μM, 10 μM, 20 μM, 30 μM, 40 μM, and 50 μM) for 24 h. CCK8 (10 μL) was added into each well for 1 h to measure absorbance values (OD) at a wavelength of 450 nm. Lethal concentration 50 (IC50) was calculated according to OD values of each well in different ivermectin concentrations. (iii) Ivermectin treatment group: 20 μM ivermectin was added to TOV-21G cells in SILAC "heavy" labeling growing medium for 24 h. Control group: 0.1% DMSO was added to TOV-21G cells in SILAC "light" labeling growing medium for 24 h.

2.4 Cell lysis and protein preparation

Ivermectin treatment and 0.1% DMSO treatment TOV-21G cells were collected and lysed by protein isolation buffer, respectively. (i) TOV-21G cells collection: A total of 500 μL trypsin was added to each 10-cm culture flasks for several minutes and collected with centrifugation (800 × g, 5 min). TOV-21G cells were washed with ice-cold phosphate buffer solution (PBS) for three times. (ii) Protein isolation buffer: 2 mM thiourea, 4% CHAPS (3-[(3-cholamidopropyl)-dimethylammonio] -1-propane), 7 M urea, 100 mM dithiothreitol (DTT), and 2% ampholyte. (iii) TOV-21G cells lysis: A total of 200 μL protein isolation buffer was added to each 10-cm culture flasks for 30 min (ice-cold) and then oscillated with five vortex cycles. (iv) SILAC-labeled protein collection: Protein isolation buffer was centrifuged (13,000 × g, 20 min, 4°C), and the SILAC-labeled protein samples were collected from the supernatants in new tubes. (v) Protein concentrations measurement: Protein concentrations of the SILAC-labeled protein samples were measured with the 2-D quant protein assay kit (Bio-Rad, US).

2.5 The preliminary experiment of SILAC-labeled protein samples

The "heavy"- and "light"-SILAC-labeled proteins were mixed and loaded onto 1X SDS-PAGE to check the quality. SDS-PAGE-separated proteins were further analyzed with MS/MS as a preliminary experiment to check the labeling efficiency. (i) The loading sample preparation: According to the 1:1 ratio, the "heavy"- and "light"-SILAC-labeled proteins were mixed in a 5X loading buffer. (ii) Electrophoresis: The mixed SILAC-labeled proteins were loaded onto SDS-PAGE gel (gel concentration: 12.5%) with the amount of 20 μg/lane by constant current (14 mA, 90 min). (iii) Coomassie brilliant blue staining: Prepare Coomassie brilliant blue stain and destain solutions. Filter the stain solution through Whatman 1 filter paper. (iv) MS/MS: Proteins were separated from SDS-PAGE bands, and then were reduced, alkylated, and trypsin-digested. The tryptic peptides were analyzed with MS/MS.

2.6 Trypsin-digestion of SILAC-labeled proteins

The main reagents and methods included: (i) Reducing agent: 100 mM DTT was added to SILAC-labeled protein sample. (ii) Uranyl acetate (UA) buffer: The UA buffer contained 8 M urea and 0.1 M Tris/HCL. The SILAC-labeled protein sample with DTT was filtered by a 10-kD ultrafiltration centrifuge tube for two times. (iii) Isolation mixture reacted: A total of 100 μL of 0.05 M iodoacetamide was added to the isolation mixture following centrifugalization (14,000 × g, 15 min). A total of 25 mM ammonium bicarbonate (NH_4HCO_3) was added to the mixture following centrifugalization (14,000 × g, 15 min). (iv) Trypsin buffer: 2 μg trypsin in 40 μL 100-mM NH_4HCO_3. (v) Tryptic peptide content: A volume of trypsin buffer (40 μL) was added to the mixture from last step and shaken by 600 rpm for 1 min. Enzymatic hydrolysis of the mixture was done for 16–18 h at 37°C. A volume (40 μL) of 25 mM NH_4HCO_3 was added to the mixture and that mixture was centrifuged (14,000 × g, 15 min); the filtrate was collected.

2.7 LC-MS/MS analysis

The instrument and materials are as follows: (i) MS instrument, for example, Q Exactive mass spectrometer (Thermo Fisher Scientific); (ii) Easy nLC system, for example, Proxeon Biosystems (Thermo Fisher Scientific); (iii) Thermo scientific EASY column: Acclaim PepMap, 100 μm × 2 cm, nanoViper, 5 μm-C18; (iv) analytical column: Thermo scientific EASY column (75 μm * 100 mm 3 μm-C18); (v) solvent A: 0.1% formic acid in H_2O; and (vi) solvent B: 0.1% formic acid, 84% acetonitrile in H_2O.

2.8 Search protein database with MaxQuant software

The main parameters are following [20]: Main search ppm: 6; missed cleavage: 2; MS/MS tolerance ppm: 20; de-isotopic: TRUE; enzyme: trypsin/P; database: uniprot_Homo_sapiens_169753_20190313; fixed modification: carbamidomethyl (C); lables: Lys(8), Arg(10); variable modification: oxidation (M), acetyl (protein N-term) decoy database; pattern: reverse; peptide FDR: 0.01; and protein FDR: 0.01.

2.9 Bioinformatics analysis

Several bioinformatics analyses were used, which are as follows: (i) The enrichment of Kyoto Encyclopedia of Genes and Genomes (KEGG) pathway was performed with R package clusterProfiler-KEGG (https://bioconductor.org/packages/release/bioc/html/clusterProfiler.html). (ii) The enrichment of biological processes (BPs) was analyzed with Cytoscape ClueGO. (iii) The level of statistical significance was set as $p < 0.05$ and adjusted p value < 0.05. For KEGG and BPs enrichment analyses, a Benjamini-Hochberg multiple text was used to adjust p value.

3. Results and discussion

3.1 Proteomic profile based on SILAC in ivermectin-treated TOV-21G cells

The flow chart of SILAC quantitative proteomics was shown to summarize the overall analysis process for the identification of ivermectin-related proteins (**Figure 1**).

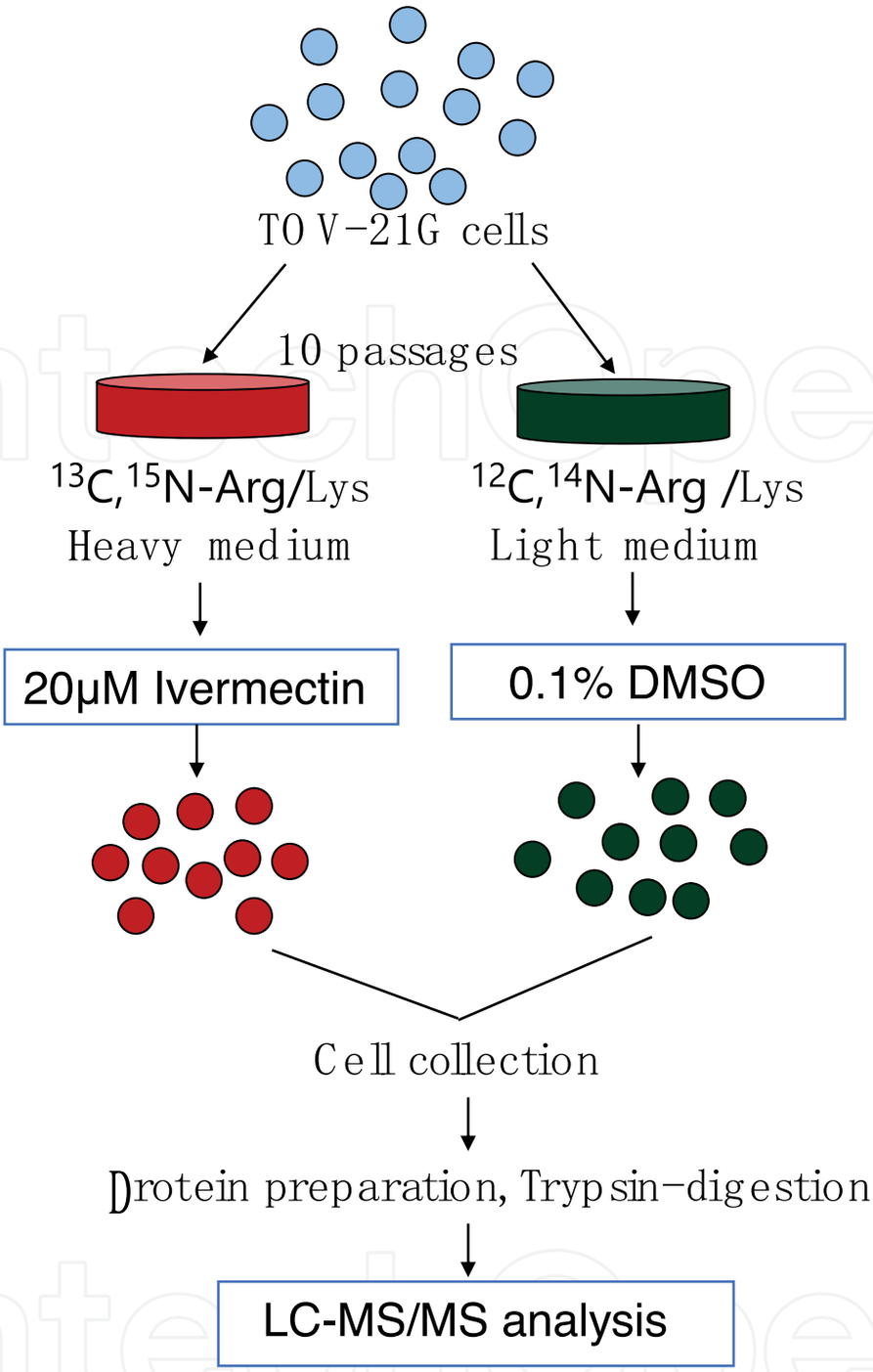

Figure 1.
The flow chart of SILAC quantitative proteomics analysis of ovarian cancer cells treated with and without ivermectin.

In total, 4447 proteins were identified with SILAC quantitative proteomics in human ovarian cancer cells treated with ivermectin. The ratio of "heavy"/"light" labeling samples was obtained, including 97.91% proteins with ratio < 1, and 2.09% proteins with ratio > 1. The MS/MS spectra of tryptic peptides EYQDLLNVK (**Figure 2A**) and VVQGSLDSLPQAVR (**Figure 2B**) are taken as examples. For peptide EYQDLLNVK (gene name = NEFM), the excellent b-ion and y-ion series were obtained with high signal-to-noise (S/N) (**Figure 2A**). For peptide VVQGSLDSLPQAVR (gene name = PKC1), the excellent b-ion and y-ion series were also obtained with high signal-to-noise (S/N) (**Figure 2B**).

The fold-changes of some identified proteins were very striking; for example, those upregulated proteins (ratio > 2), including histone H2A, progranulin,

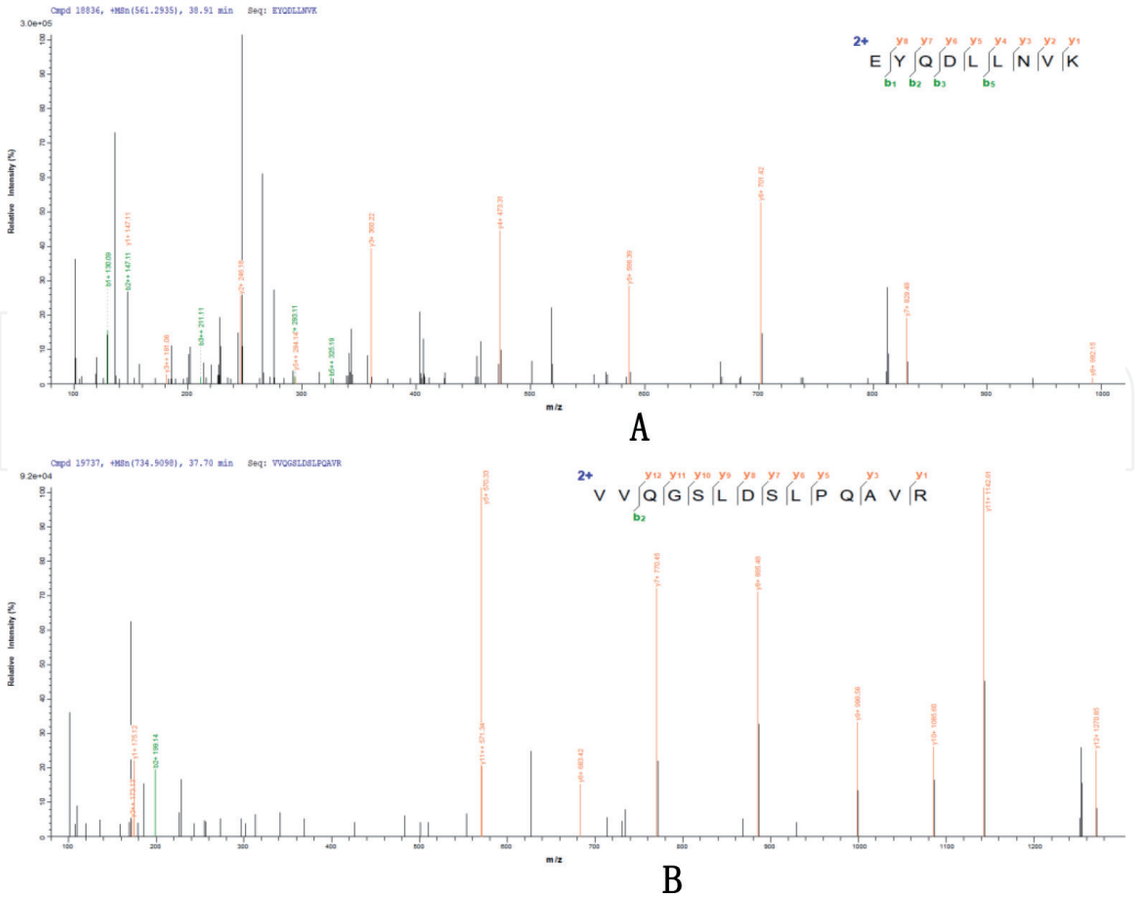

Figure 2.
The MS/MS spectra of tryptic peptides with SILAC labeling. (A) MS/MS spectrum of tryptic peptide EYQDLLNVK (gene name = NEFM). (B) MS/MS spectrum of tryptic peptide VVQGSLDSLPQAVR (gene name = PKC1).

cathepsin Z, SWI/SNF-related matrix-associated actin-dependent regulator of chromatin subfamily A-like protein 1, beta-mannosidase, GRAM domain-containing 1C, BMP-2-inducible protein kinase, ribosomal protein L3, ubiquitin-conjugating enzyme E2, PIK3R1, LIM domain-containing protein 1, retinal guanylyl cyclase 1, telomerase-binding protein EST1A, and COX7A2L protein. Some of them have been reported in ovarian cancers. For example, recent studies demonstrated that PI3K/AKT/mTOR and ERK1/2 signaling pathways were involved in this chemo-resistance. Progranulin was upregulated in epithelial ovarian cancer cell lines and associated with cisplatin resistance through regulating AKT/mTOR and ERK1/2 signaling pathways [21]. Progranulin is also involved in the process of cartilage development, progression, wound healing, and inflammation in ovarian cancer [22]. Additionally, one study showed that progranulin could directly activate cancer-associated fibroblasts to induce the epithelial-mesenchymal transition process of epithelial ovarian cancer cells [23]. Copy number loss of PIK3R1 most commonly occurs in ovarian cancer, which would activate AKT and p110-independent JAK2/STAT3 signaling and renders ovarian cancer cells vulnerable to AKT inhibitors [24]. CD97 can activate NF-κB-dependent JAK2/STAT3 pathway, consequently playing an important role in migratory, invasive capacity, and drug-resistant in ovarian cancer cells [25].

Some downregulated proteins (ratio < 0.1) were also very striking; for example, anion exchange protein, Rho guanine nucleotide exchange factor 16, dynein assembly factor 1, glucoside xylosyltransferase 1, glutamine synthetase, insulin-like growth factor-binding protein 2, microtubule-associated protein RP/EB family member 3, myelin proteolipid protein, neurochondrin, neurofilament medium

polypeptide, phosphoenolpyruvate carboxykinase, ANKUB1, and TASOR 2. Some of them play an important role in the pathogenesis of ovarian cancer. For example, the most prominent effects of insulin-like growth factor-binding protein 2 in ovarian cancer include promoting driving invasion, proliferation, and suppressing apoptosis. The area under the ROC curve of insulin-like growth factor-binding protein 2 in detecting ovarian cancer was 0.815 (95% CI: 0.721–0.910, $P < 0.001$), further studies are needed to confirm its diagnostic performance at an early stage of ovarian cancer [26].

The glutamine metabolism could be a novel therapeutic target against cisplatin resistance in various cancers. Glutamine synthetase can take part in the reprogramming of glutamine metabolism to induce cisplatin resistance in A2780 ovarian cancer cells [27]. Anion exchanger 2 is a sodium-independent chloride/bicarbonate transporter, which is implicated in the regulation of membrane potential and intracellular potential of hydrogen (pH value). Anion exchanger 2 was highly expressed in ovarian cancer tissues compared to adjacent non-tumor lesions with quantitative proteomics analysis [28]. Those identified proteins in ovarian cancer cells treated with and without ivermectin with SILAC quantitative proteomics discovered reliable and effective biomarkers and drug targets for the anticancer process of ivermectin [8].

3.2 Ivermectin-mediated molecular pathway in human ovarian cancer cells

In total, 89 statistically significant molecular pathways were enriched based on those 4447 ivermectin-related proteins with KEGG pathway analysis (**Table 1**).

These molecular pathways demonstrated that ivermectin was involved in multiple cancer-related molecular pathways, such as mismatch repair process, ErbB signaling pathway, HIF-1 signaling pathway, cell-cycle regulation, ubiquitin-mediated proteolysis, AMPK signaling pathway, apoptosis, ferroptosis, proteoglycans, and central carbon metabolism in cancer. These molecular pathways also indicated that ivermectin was involved in multiple cancer pathogenesis, such as energy metabolism pathways, immunity-related pathways, stromal element-related pathways, RNA regulation pathways, hormone signaling pathways, and biosynthesis of substances. Different pathways enriched different proteins, whereas some pathways shared the same proteins. These data showed that ivermectin has a complex influence on various signaling pathways. The results were consistent with many studies previously. Ivermectin induced PAK1-mediated cytostatic autophagy both *in vitro* and *in vivo*, which might be one of the PAK1 inhibitors and inhibits the growth of ovarian cancer, glioblastoma, breast cancer, and NF2 tumors [29]. Another investigation found that ivermectin induced apoptosis in HeLa cells by upregulating Bax and p53 expressions, enhancing cytochrome c release, decreasing the levels of CDK2, CDK6, cyclin E, and cyclin D1 [30]. The primary immunogenic features—immunogenic cell death (ICD) included the release of high-mobility-group protein B1, secreted ATP, and surface-exposed calreticulin. Recent data supported that ivermectin could kill human triple-negative breast cancer cells through mechanisms of ICD, which induced pannexin-1 channel opening and cell death [31]. Ivermectin was also reported as an RNA helicase inhibitor, which reduced precursor and mature microRNAs potentially inhibiting cell invasion and proliferation [32]. Additionally, ivermectin effectively targets angiogenesis through decreasing membrane potential, mitochondrial respiration, ATP levels, and increasing mitochondrial superoxide, and the effects proliferation, capillary network formation, and survival in human brain microvascular endothelial cell [33]. According to the cross-talking between different signaling pathways, more favorable evidence indicated that ivermectin in combination with other drugs

Pathway ID	Pathway name	p value
hsa00010	Glycolysis/gluconeogenesis	2.03E−03
hsa00020	Citrate cycle (TCA cycle)	7.38E−11
hsa00030	Pentose phosphate pathway	3.51E−04
hsa00052	Galactose metabolism	6.04E−03
hsa00062	Fatty acid elongation	1.09E−02
hsa00071	Fatty acid degradation	1.39E−05
hsa00190	Oxidative phosphorylation	3.47E−12
hsa00230	Purine metabolism	1.08E−02
hsa00240	Pyrimidine metabolism	2.55E−03
hsa00270	Cysteine and methionine metabolism	8.93E−07
hsa00280	Valine, leucine and isoleucine degradation	2.06E−08
hsa00480	Glutathione metabolism	1.05E−03
hsa00510	N-Glycan biosynthesis	4.31E−03
hsa00513	Various types of N-glycan biosynthesis	5.15E−03
hsa00520	Amino sugar and nucleotide sugar metabolism	1.04E−07
hsa00620	Pyruvate metabolism	1.11E−07
hsa00630	Glyoxylate and dicarboxylate metabolism	4.09E−03
hsa00640	Propanoate metabolism	1.16E−05
hsa00920	Sulfur metabolism	4.45E−03
hsa01040	Biosynthesis of unsaturated fatty acids	1.09E−02
hsa01200	Carbon metabolism	3.96E−16
hsa01212	Fatty acid metabolism	1.74E−08
hsa01230	Biosynthesis of amino acids	3.09E−08
hsa03008	Ribosome biogenesis in eukaryotes	3.34E−04
hsa03010	Ribosome	7.07E−22
hsa03013	RNA transport	8.04E−20
hsa03015	mRNA surveillance pathway	4.28E−08
hsa03018	RNA degradation	2.24E−07
hsa03030	DNA replication	8.18E−09
hsa03040	Spliceosome	5.79E−24
hsa03050	Proteasome	1.50E−14
hsa03410	Base excision repair	1.22E−02
hsa03420	Nucleotide excision repair	4.72E−06
hsa03430	Mismatch repair	4.33E−04
hsa04012	ErbB signaling pathway	6.27E−03
hsa04066	HIF-1 signaling pathway	1.31E−05
hsa04071	Sphingolipid signaling pathway	9.01E−03
hsa04110	Cell cycle	4.03E−03
hsa04120	Ubiquitin mediated proteolysis	1.82E−06
hsa04130	SNARE interactions in vesicular transport	1.18E−04
hsa04137	Mitophagy—animal	9.07E−03

Pathway ID	Pathway name	p value
hsa04141	Protein processing in the endoplasmic reticulum	1.07E−13
hsa04142	Lysosome	3.81E−06
hsa04144	Endocytosis	9.24E−15
hsa04145	Phagosome	8.66E−07
hsa04152	AMPK signaling pathway	3.49E−03
hsa04210	Apoptosis	1.07E−03
hsa04213	Longevity regulating pathway—multiple species	4.46E−03
hsa04216	Ferroptosis	4.75E−04
hsa04510	Focal adhesion	2.57E−05
hsa04520	Adherens junction	2.04E−05
hsa04530	Tight junction	6.21E−05
hsa04540	Gap junction	3.14E−03
hsa04611	Platelet activation	4.03E−03
hsa04666	Fc gamma R-mediated phagocytosis	2.41E−03
hsa04714	Thermogenesis	1.08E−09
hsa04720	Long-term potentiation	7.22E−03
hsa04721	Synaptic vesicle cycle	2.29E−04
hsa04810	Regulation of actin cytoskeleton	4.94E−06
hsa04910	Insulin signaling pathway	2.90E−04
hsa04919	Thyroid hormone signaling pathway	5.20E−03
hsa04922	Glucagon signaling pathway	3.38E−04
hsa04931	Insulin resistance	1.26E−02
hsa04932	Nonalcoholic fatty liver disease (NAFLD)	1.44E−07
hsa04961	Endocrine and other factor-regulated calcium reabsorption	1.83E−03
hsa04962	Vasopressin-regulated water reabsorption	9.81E−03
hsa05010	Alzheimer disease	3.09E−07
hsa05012	Parkinson disease	5.32E−23
hsa05014	Amyotrophic lateral sclerosis (ALS)	2.55E−03
hsa05016	Huntington disease	7.93E−13
hsa05100	Bacterial invasion of epithelial cells	5.95E−10
hsa05110	*Vibrio cholerae* infection	6.22E−06
hsa05120	Epithelial cell signaling in *Helicobacter pylori* infection	1.07E−04
hsa05130	Pathogenic *Escherichia coli* infection	6.13E−09
hsa05131	Shigellosis	2.10E−07
hsa05132	Salmonella infection	7.10E−14
hsa05134	Legionellosis	1.05E−03
hsa05135	Yersinia infection	4.64E−06
hsa05163	Human cytomegalovirus infection	5.57E−05
hsa05165	Human papillomavirus infection	4.68E−03
hsa05169	Epstein-Barr virus infection	2.03E−05

Pathway ID	Pathway name	p value
hsa05170	Human immunodeficiency virus 1 infection	4.59E−08
hsa05203	Viral carcinogenesis	6.98E−05
hsa05205	Proteoglycans in cancer	2.44E−05
hsa05211	Renal cell carcinoma	2.65E−03
hsa05212	Pancreatic cancer	6.79E−03
hsa05220	Chronic myeloid leukemia	1.31E−02
hsa05230	Central carbon metabolism in cancer	1.18E−03
hsa03060	Protein export	8.73E−05

Table 1.
Statistically significant pathways identified with ivermectin-related proteins with KEGG pathway enrichment analysis.

exhibited more powerful anticancer effects, including daunorubicin, anti-BRAF V600 inhibitors, cytarabine, paclitaxel, and tamoxifen [34]. Obviously, the detailed mechanisms of ivermectin remain unclear. However, the application of new drugs brought ones to better health.

3.3 Ivermectin-mediated biological processes in human ovarian cancer cells

A total of 61 statistically significant biological processes were enriched based on those 4447 ivermectin-related proteins with GO analysis (**Figure 3**). These biological processes indicated that ivermectin was involved in multiple cancer-related biological processes, such as negative/positive regulation of canonical Wnt signaling pathway, cysteine-type endopeptidase activity involved in the apoptotic process, innate immune response-activating signal transduction, protein targeting to membrane, T-cell receptor signaling pathway, regulation of protein ubiquitination, activation of protein kinase activity, regulation of transcription by RNA polymerase II, and DNA-binding transcription factor activity. These results were consistent with many studies previously. For example, CTNNB1 (catenin beta 1, IMPβ1) in the biological process of protein polyubiquitination, was responsible for the nuclear entry of cargoes. Ivermectin can impact thermal stability and α-helicity of IMPα and IMPβ1 by binding to the IMPα armadillo repeat domain [35]. CASP3 in the biological process of protein kinase regulator activity is a member of the cysteine-aspartic acid protease (caspase) family. SK-MEL-28 cells were treated with different concentrations of ivermectin (2.5 μM, 5 μM, and 10 μM). Ivermectin enhanced the apoptosis effect by the upregulation of caspase-3 activity [36]. Also, PAK1 in the biological process of protein kinase regulator activity binds to and inhibits the activity of cyclin-cyclin-dependent kinase 2 or -cyclin-dependent kinase 4 complexes, and thus functions as a regulator of cell-cycle progression at G1. Ivermectin inhibited cancer stem cells formation by regulating the binding of PAK1/Stat3 complex and the IL-6 promoter [37]. YAP1 in the biological process of positive regulation of canonical Wnt signaling pathway was involved in the development, growth, repair, and homeostasis of multiple cancers. Ivermectin inhibited YAP1 nuclear expression and nuclear accumulation in gastric cancer cells. Moreover, in xenografts of gastric cancer cells, ivermectin suppressed tumor growth by regulating YAP1 nuclear expression [38]. Those identified proteins in ovarian cancer cells treated with and without ivermectin based on the SILAC method play important roles in multiple cellular signaling pathways and have broad biological activities. Those findings provide basic data for further study of ivermectin in ovarian cancer.

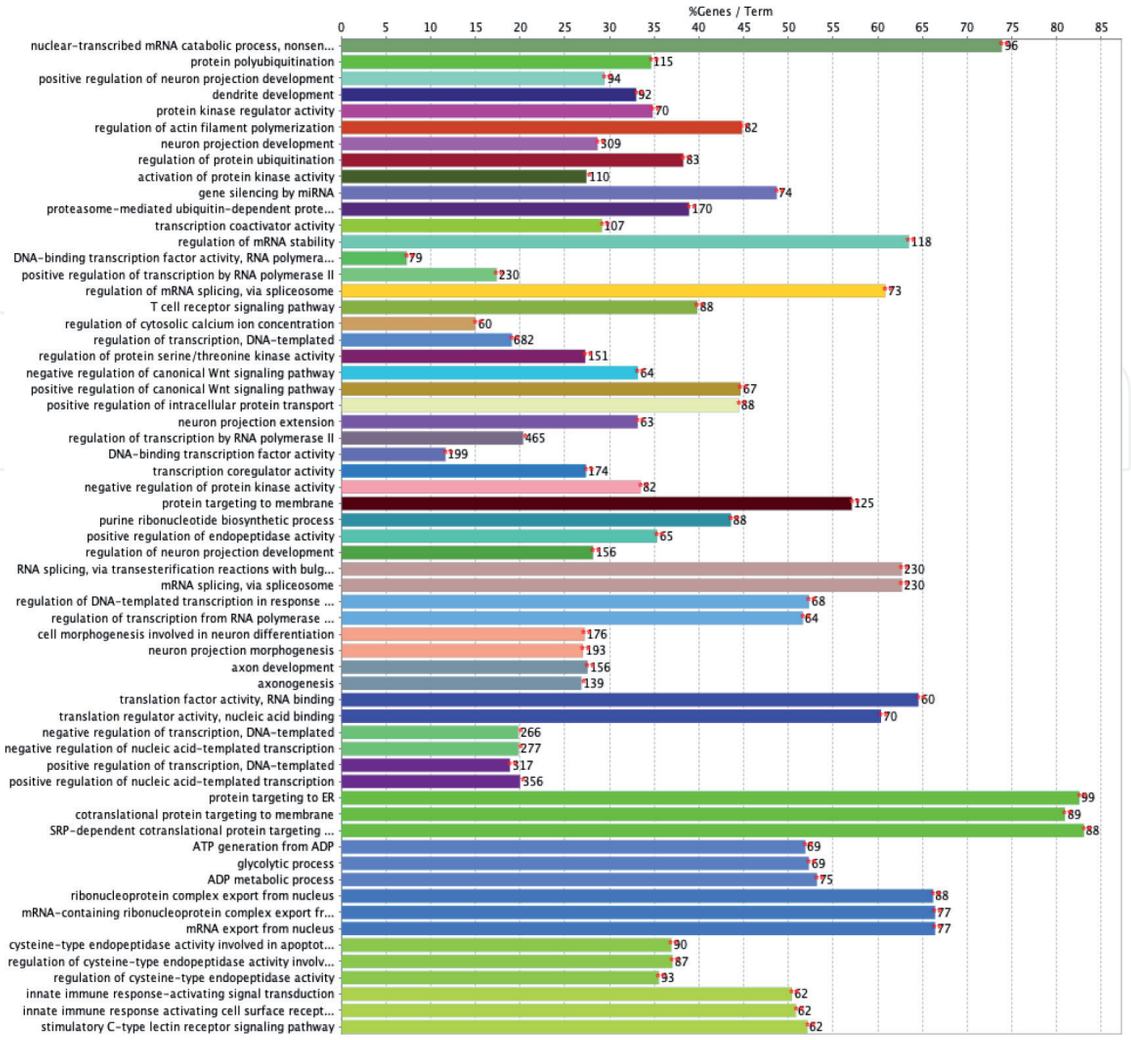

Figure 3.
Statistically significant biological processes (BPs) identified with ivermectin-related proteins with GO enrichment analysis.

4. Conclusions

Stable isotope labeling with amino acids in cell culture (SILAC) was an effective quantitative proteomics method to identify differentially expressed proteins or differentially modified proteins in cultured cells between two different conditions. In this study, ovarian cancer cells TOV-21 under two different conditions were cultured with the "heavy" labeling medium that contained 50 mg L-lysine-2HCl [^{13}C6, ^{15}N2] and 50 mg L-arginine-HCl [^{13}C6, ^{15}N4] in 500 mL RPMI 1640 medium, and the "light" labeling medium that contained 50 mg L-lysine-2HCl [^{12}C6, ^{14}N2] and 50 mg L-arginine-HCl [^{12}C6, ^{14}N4] in 500 mL RPMI 1640 medium for 10 passages, respectively. Then TOV-21G cells with SILAC "heavy" or "light" labeling were treated with or without 20 μM ivermectin for 24 h. The heavy- and light-stable isotope-labeled proteins were equally mixed (1:1), digested with trypsin, and analyzed with LC-MS/MS. A total of 4447 proteins were identified in ivermectin-treated TOV-21G cells relative to controls, and these proteins were significantly enriched in 89 molecular pathways, and 62 biological processes. These findings offer important data to study ivermectin-mediated molecular pathway network changes and discover effective ivermectin-related biomarkers and therapeutic targets for ivermectin treatment of ovarian cancer.

Acknowledgements

The authors acknowledge the financial supports from the Shandong First Medical University Talent Introduction Funds (to X.Z.), and the Hunan Provincial Hundred Talent Plan (to X.Z.).

Author's contributions

N.L. analyzed the data, prepared figures, and wrote the manuscript. X.Z. conceived the concept, designed the manuscript, wrote and critically revised the manuscript, and was responsible for the correspondence work and financial support.

Conflict of interest

We declare that we have no financial and personal relationships with other people or organizations.

Acronyms and abbreviations

BPs	biological processes
CTNNB1	catenin beta 1
ICD	immunogenic cell death
DTT	dithiothreitol
EGFR	epidermal growth factor receptor
IC50	lethal concentration 50
KEGG	Kyoto Encyclopedia of Genes and Genomes
LC	liquid chromatography
MS	mass spectrometry
MS/MS	tandem mass spectrometry
OD	absorbance values
PBS	phosphate buffer solution
SILAC	stable isotope labeling with amino acids in cell culture

Author details

Na Li[1,2] and Xianquan Zhan[1,2,3]*

1 Shandong Key Laboratory of Radiation Oncology, Shandong Cancer Hospital and Institute, Shandong First Medical University, Jinan, Shandong, P.R. China

2 Medical Science and Technology Innovation Center, Shandong First Medical University, Jinan, Shandong, P.R. China

3 Gastroenterology Research Institute and Clinical Center, Shandong First Medical University, Jinan, Shandong, P.R. China

*Address all correspondence to: yjzhan2011@gmail.com

References

[1] Chen X, Wei S, Ji Y, Guo X, Yang F. Quantitative proteomics using SILAC: Principles, applications, and developments. Proteomics. 2015;**15**(18): 3175-3192. DOI: 10.1002/pmic.201500108

[2] Deng J, Erdjument-Bromage H, Neubert TA. Quantitative comparison of proteomes using SILAC. Current Protocols in Protein Science. 2019;**95**(1):e74. DOI: 10.1002/cpps.74

[3] Hoedt E, Zhang G, Neubert TA. Stable isotope labeling by amino acids in cell culture (SILAC) for quantitative proteomics. Advances in Experimental Medicine and Biology. 2019;**1140**:531-539. DOI: 10.1007/978-3-030-15950-4_31

[4] Ong SE. The expanding field of SILAC. Analytical and Bioanalytical Chemistry. 2012;**404**(4):967-976. DOI: 10.1007/s00216-012-5998-3

[5] Stepath M, Zülch B, Maghnouj A, et al. Systematic comparison of label-free, SILAC, and TMT techniques to study early adaption toward inhibition of EGFR signaling in the colorectal cancer cell line DiFi. Journal of Proteome Research. 2020;**19**(2):926-937. DOI: 10.1021/acs.jproteome.9b00701

[6] Kaeser-Pebernard S, Diedrich B, Dengjel J. Identification and regulation of multimeric protein complexes in autophagy via SILAC-based mass spectrometry approaches. Methods in Molecular Biology. 2019;**1880**:341-357. DOI: 10.1007/978-1-4939-8873-0_23

[7] Tackett AJ, DeGrasse JA, Sekedat MD, et al. I-DIRT, a general method for distinguishing between specific and nonspecific protein interactions. Journal of Proteome Research. 2005;**4**(5):1752-1756. DOI: 10.1021/pr050225e

[8] Li N, Li J, Desiderio DM, Zhan X. SILAC quantitative proteomics analysis of ivermectin-related proteomic profiling and molecular network alterations in human ovarian cancer cells. Journal of Mass Spectrometry. 2021;**56**(1):e4659. DOI: 10.1002/jms.4659

[9] Snider J, Wang D, Bogenhagen DF, Haley JD. Pulse SILAC approaches to the measurement of cellular dynamics. Advances in Experimental Medicine and Biology. 2019;**1140**:575-583. DOI: 10.1007/978-3-030-15950-4_34

[10] Savitski MM, Zinn N, Faelth-Savitski M, et al. Multiplexed proteome dynamics profiling reveals mechanisms controlling protein homeostasis. Cell. 2018;**173**(1):260-274.e25. DOI: 10.1016/j.cell.2018.02.030

[11] Crump A. Ivermectin: Enigmatic multifaceted 'wonder' drug continues to surprise and exceed expectations. Journal of Antibiotics (Tokyo). 2017;**70**(5):495-505. DOI: 10.1038/ja.2017.11

[12] Develoux M. Ivermectin. Annales de Dermatologie et de Vénéréologie. 2004;**131**(6-7 Pt 1):561-570. DOI: 10.1016/s0151-9638(04)93668-x

[13] Levy M, Martin L, Bursztejn AC, et al. Ivermectin safety in infants and children under 15 kg treated for scabies: A multicentric observational study. The British Journal of Dermatology. 2020;**182**(4):1003-1006. DOI: 10.1111/bjd.18369

[14] Nicolas P, Maia MF, Bassat Q, et al. Safety of oral ivermectin during pregnancy: A systematic review and meta-analysis. The Lancet Global Health. 2020;**8**(1):e92-e100. DOI: 10.1016/s2214-109x(19)30453-x

[15] Guzzo CA, Furtek CI, Porras AG, et al. Safety, tolerability, and

pharmacokinetics of escalating high doses of ivermectin in healthy adult subjects. Journal of Clinical Pharmacology. 2002;**42**(10):1122-1133. DOI: 10.1177/009127002401382731

[16] Dou Q, Chen HN, Wang K, et al. Ivermectin Induces Cytostatic Autophagy by Blocking the PAK1/Akt Axis in Breast Cancer. Cancer Research. 2016;**76**(15):4457-4469. DOI: 10.1158/0008-5472.Can-15-2887

[17] Sharmeen S, Skrtic M, Sukhai MA, et al. The antiparasitic agent ivermectin induces chloride-dependent membrane hyperpolarization and cell death in leukemia cells. Blood. 2010;**116**(18):3593-3603. DOI: 10.1182/blood-2010-01-262675

[18] Li N, Zhan X. Anti-parasite drug ivermectin can suppress ovarian cancer by regulating lncRNA-EIF4A3-mRNA axes. The EPMA Journal. 2020;**11**(2):289-309. DOI: 10.1007/s13167-020-00209-y

[19] Li N, Li H, Wang Y, Cao L, Zhan X. Quantitative proteomics revealed energy metabolism pathway alterations in human epithelial ovarian carcinoma and their regulation by the antiparasite drug ivermectin: Data interpretation in the context of 3P medicine. The EPMA Journal. 2020;**11**(4):661-694. DOI: 10.1007/s13167-020-00224-z

[20] Trautwein-Schult A, Bartel J, Maaß S, Becher D. Metabolic labeling of clostridioides difficile proteins. Methods in Molecular Biology. 2021;**2228**:271-282. DOI: 10.1007/978-1-0716-1024-4_19

[21] Perez-Juarez CE, Arechavaleta-Velasco F, Zeferino-Toquero M, et al. Inhibition of PI3K/AKT/mTOR and MAPK signaling pathways decreases progranulin expression in ovarian clear cell carcinoma (OCCC) cell line: A potential biomarker for therapy response to signaling pathway inhibitors. Medical Oncology. 2019;**37**(1):4. DOI: 10.1007/s12032-019-1326-5

[22] Yang D, Wang LL, Dong TT, et al. Progranulin promotes colorectal cancer proliferation and angiogenesis through TNFR2/Akt and ERK signaling pathways. American Journal of Cancer Research. 2015;**5**(10):3085-3097

[23] Dong T, Yang D, Li R, et al. PGRN promotes migration and invasion of epithelial ovarian cancer cells through an epithelial mesenchymal transition program and the activation of cancer associated fibroblasts. Experimental and Molecular Pathology. 2016;**100**(1):17-25. DOI: 10.1016/j.yexmp.2015.11.021

[24] Li X, Mak VCY, Zhou Y, et al. Deregulated Gab2 phosphorylation mediates aberrant AKT and STAT3 signaling upon PIK3R1 loss in ovarian cancer. Nature Communications. 2019;**10**(1):716. DOI: 10.1038/s41467-019-08574-7

[25] Park GB, Kim D. MicroRNA-503-5p inhibits the CD97-mediated JAK2/STAT3 pathway in metastatic or paclitaxel-resistant ovarian cancer cells. Neoplasia. 2019;**21**(2):206-215. DOI: 10.1016/j.neo.2018.12.005

[26] Prayudi PKA, Budiana ING, Mahayasa PD, et al. Diagnostic accuracy of serum insulin-like growth factor-binding protein 2 for ovarian cancer. International Journal of Gynecological Cancer. 2020;**30**(11):1762-1767. DOI: 10.1136/ijgc-2020-001479

[27] Guo J, Satoh K, Tabata S, et al. Reprogramming of glutamine metabolism via glutamine synthetase silencing induces cisplatin resistance in A2780 ovarian cancer cells. BMC Cancer. 2021;**21**(1):174. DOI: 10.1186/s12885-021-07879-5

[28] Zhang LJ, Lu R, Song YN, et al. Knockdown of anion exchanger 2

suppressed the growth of ovarian cancer cells via mTOR/p70S6K1 signaling. Scientific Reports. 2017;**7**(1):6362. DOI: 10.1038/s41598-017-06472-w

[29] Wang K, Gao W, Dou Q, et al. Ivermectin induces PAK1-mediated cytostatic autophagy in breast cancer. Autophagy. 2016;**12**(12):2498-2499. DOI: 10.1080/15548627.2016.1231494

[30] Song D, Liang H, Qu B, et al. Ivermectin inhibits the growth of glioma cells by inducing cell cycle arrest and apoptosis in vitro and in vivo. Journal of Cellular Biochemistry. 2019;**120**(1):622-633. DOI: 10.1002/jcb.27420

[31] Draganov D, Gopalakrishna-Pillai S, Chen YR, et al. Modulation of P2X4/P2X7/pannexin-1 sensitivity to extracellular ATP via ivermectin induces a non-apoptotic and inflammatory form of cancer cell death. Scientific Reports. 2015;**5**:16222. DOI: 10.1038/srep16222

[32] Yin J, Park G, Lee JE, et al. DEAD-box RNA helicase DDX23 modulates glioma malignancy via elevating miR-21 biogenesis. Brain. 2015;**138**(Pt 9):2553-2570. DOI: 10.1093/brain/awv167

[33] Liu Y, Fang S, Sun Q, Liu B. Anthelmintic drug ivermectin inhibits angiogenesis, growth and survival of glioblastoma through inducing mitochondrial dysfunction and oxidative stress. Biochemical and Biophysical Research Communications. 2016;**480**(3):415-421. DOI: 10.1016/j.bbrc.2016.10.064

[34] Liu J, Zhang K, Cheng L, Zhu H, Xu T. Progress in Understanding the Molecular Mechanisms Underlying the Antitumour Effects of Ivermectin. Drug Design, Development and Therapy. 2020;**14**:285-296. DOI: 10.2147/dddt.S237393

[35] Yang SNY, Atkinson SC, Wang C, et al. The broad spectrum antiviral ivermectin targets the host nuclear transport importin α/β1 heterodimer. Antiviral Research. 2020;**177**:104760. DOI: 10.1016/j.antiviral.2020.104760

[36] Deng F, Xu Q, Long J, Xie H. Suppressing ROS-TFE3-dependent autophagy enhances ivermectin-induced apoptosis in human melanoma cells. Journal of Cellular Biochemistry. 2018. DOI: 10.1002/jcb.27490

[37] Kim JH, Choi HS, Kim SL, Lee DS. The PAK1-Stat3 signaling pathway activates IL-6 gene transcription and human breast cancer stem cell formation. Cancers (Basel). 2019;**11**(10):1527. DOI: 10.3390/cancers11101527

[38] Nambara S, Masuda T, Nishio M, et al. Antitumor effects of the antiparasitic agent ivermectin via inhibition of Yes-associated protein 1 expression in gastric cancer. Oncotarget. 2017;**8**(64):107666-107677. DOI: 10.18632/oncotarget.22587